Lab on a Chip

Accepted Manuscript

ROYAL SOCIETY OF CHEMISTRY

www.rsc.org/loc

Graphical abstract

A fiber-shaped cellular constructs of human iPS-derived cardiomyocyte to quantify the contractile force for analyses of their drug reactivity.

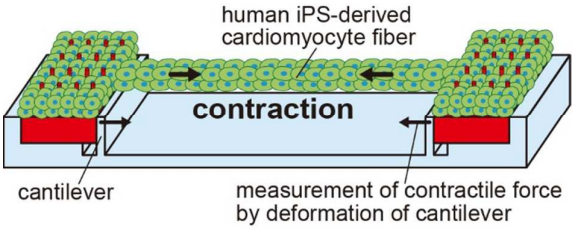

Journal Name

ARTICLE

Human induced pluripotent stem cell-derived fiber-shaped cardiac tissue on a chip

Received 00th January 20xx,
Accepted 00th January 20xx

DOI: 10.1039/x0xx00000x

www.rsc.org/

Y. Morimoto[a, b], S. Mori[a, b], F. Sakai[a, b] and S. Takeuchi[*a, b]

We propose a method for the production of a fiber-shaped three-dimensional (3D) cellular construct of human induced pluripotent stem cell-derived cardiomyocytes (hiPS-CMs) for the quantification of the contractile force. By culturing the cardiomyocytes in a patterned hydrogel structure with fixed edges, we succeeded in the fabrication of hiPS-CM fibers with aligned cardiomyocytes. The fiber generated contractile force along the fiber direction due to the hiPS-CM alignment, and we were able to measure its contractile force accurately. Furthermore, to demonstrate the drug reactivity of hiPS-CM fibers, the changes in the contractile frequency and force following treatment with isoproterenol and propranolol were observed. We believe that hiPS-CM fibers will be a useful tool for pharmacokinetic analyses during drug development.

Introduction

Due to the recent advancements in the development of human pluripotent stem cells, such as human embryonic stem cells (hESCs) and human induced pluripotent stem cells (hiPSCs), human cardiomyocytes (CMs) have been available for analyses of human cardiac physiology in vitro [1]. For the investigations of cardiac morphology, functions, and drug responses, construction of human CM model systems is necessary [2].

Conventional methods used for the evaluation of cardiac properties include two-dimensional (2D) monolayer cardiac culture in culture dishes [3-7], multi-electrode arrays [6-8], and microsized post arrays [9-13]. These techniques are used for image analyses, the characterization of electrophysiological effects, and contractile force measurements at the single-cell level, respectively. Since 2D monolayer cardiac cultures lack the rich cell-cell and cell-extracellular matrix (ECM) interactions and limited contractile motions, the proper cardiac morphology and functions cannot be established. Therefore, CMs may weaken myofibrillogenesis and sarcomeric banding, causing the loss of sensitivity to certain physiologic stimulations such as hormone [14, 15].

Many researchers have proposed the development of three-dimensional (3D) cardiac cellular constructs fabricated by culturing CMs with synthetic substrate [16-18] and biodegradable hydrogels such as ECMs [19-23] in order to solve this problem. CM cultures in hydrogel structures have potentials to achieve the improved in vitro model systems for the analyses of cardiac tissues because they allow cell-cell and cell-ECM interactions and application of mechanical stress by the fixation of their edges with anchors. Additionally, this method enables the evaluation of contractile force of 3D human iPS-derived CM (hiPS-CM) constructs by cantilever integration [22, 23]. However, it is difficult to control the shapes of 3D cardiac cellular constructs when culturing CMs in large hydrogel structure because of the non-uniform shrinkage of the constructs due to the traction force of sparsely dispersed CMs in the hydrogel structures. The control of CM orientation in the cardiac cellular constructs is also difficult to achieve without any additional stimulations such as cyclic stretch and chronic electrical stimulations [14, 23] because the orientation of cells in these structures depends on the shapes of 3D cellular constructs [24].

Here, we propose a method for the generation of a fiber-shaped cellular construct of hiPS-CMs by patterning of the hydrogel structures with hiPS-CMs (Fig. 1(i)). This method enables us to control the shapes of hiPS-CM fibers by an initial shaping of the hydrogel structures containing highly dense hiPS-CMs in a fiber-like shape. This high cellular density prevents an extensive shrinkage of the construct. Additionally, the formation of a narrow-shaped hydrogel structure allows the alignment of hiPS-CMs along the direction of the fiber. Due to this alignment, the fibers are able to contract along this direction. Upon the transfer of the fibers to the substrates with cantilevers, we can estimate their contractile force from cantilever deformation; the estimation of contractile force after the application of various drugs for human bodies allows us to detect drug reactivity of the hiPS-CM fibers. The detection of drug reactivity based on contractile force of the hiPS-CM fiber will be useful for the development of drugs targeting human cardiac diseases and for the analyses of adverse effects of these drugs.

[a] Center for International Research on Integrative Biomedical Systems (CIBiS), Institute of Industrial Science (IIS), The University of Tokyo, 4-6-1 Komaba, Meguro-ku, Tokyo, 153-8505, Japan.
[b] Takeuchi biohybrid Innovation Project, ERATO, Japan Science and Technology (JST), Komaba Open Laboratory (KOL) Room M202, 4-6-1, Komaba, Meguro-ku, Tokyo, 153-8904, Japan.
Electronic Supplementary Information (ESI) available: See DOI: 10.1039/x0xx00000x

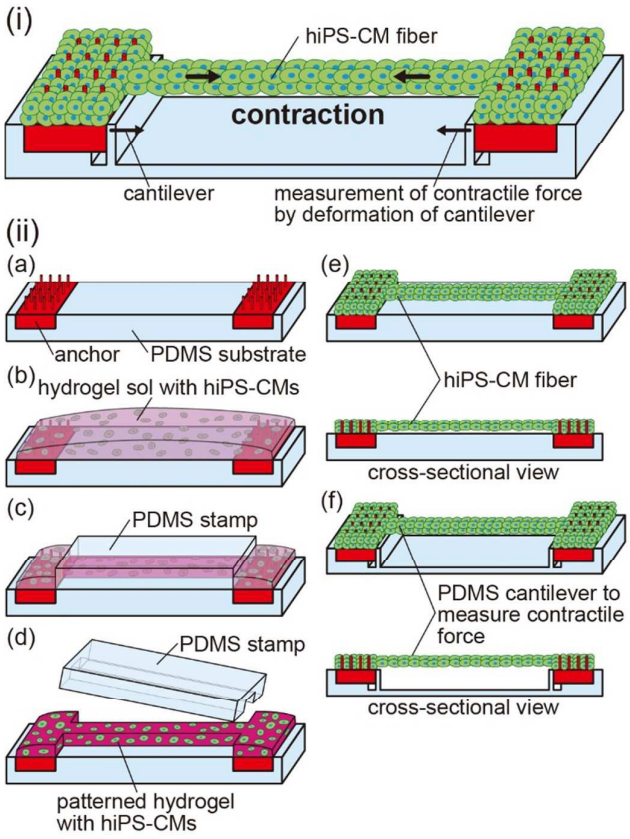

Fig. 1 (i) Schematic illustration of the contractile force measurements of the hiPS-CM fiber. The contractile force was estimated from the cantilever deformation. (ii) Schematic illustration of hiPS-CM fiber fabrication process. (a) Arrangement of the anchors with pillars on a PDMS substrate. (b) Placement of a pre-gel solution containing hiPS-CMs on the anchors and the substrate. (c) Sandwiching the pre-gel solution using a PDMS stamp. (d) Releasing the PDMS stamp after gelation of pre-gel solution. (e) Formation of the hiPS-CM fibers by culturing hiPS-CMs. (f) Transfer of the hiPS-CM fibers to a substrate with cantilevers.

Materials and methods

Cell preparation

HiPS-CMs (iCell Cardiomyocytes, Cellular Dynamics International, Inc., (CDI)) were seeded and maintained according to the manufacturer's instructions, using iCell Cardiomyocytes Plating Medium and iCell Cardiomyocytes Maintenance Medium (CDI) at 37°C in a 5% CO2 atmosphere. These cells were collected from the culture dishes following a treatment with TrypLE (Gibco TrypLE Select, Thermo Fisher Scientific, Inc.).

Fabrication of iPS-derived cardiomyocyte fibers

In order to generate hiPS-CM fibers, we prepared anchors with pillars, a polydimethylsiloxane (PDMS) stamp, and a PDMS substrate. For the preparation of anchors, we used a commercial stereolithography machine (Perfactory; EnvisionTEC) with photoreactive acrylate resin (R11, 25-50 µm layers; EnvisionTEC). Following the formation of the anchors, we exposed them to ultraviolet (UV) light for over 60 s using a laser machine (UV-LED; Keyence Corp.) for complete curing. Afterward, we coated them with 2 µm parylene using a chemical vapor deposition machine (Parylene Deposition System 2010; Specialty Coating Systems, Inc.). After the anchors have been exposed to UV light for over 10 h in order to sterilize them, we coated them with fibronectin (Stabilized bovine fibronectin; Thermo Fisher Scientific Inc.) to enable cell adhesion.

For the preparation of PDMS stamp and substrate, we used resin molds in order to shape them. The resin molds were fabricated by the same method as the anchors using the stereolithography machine. After the exposure to UV light and parylene coating, we poured PDMS elastomer (Sylgard 184 Silicone Elastomer; Dow Corning Toray Co., Ltd.) mixed in the ratio of 10:1 (base/cross-linker) into the resin molds. We heated them for 90 min at 75°C to solidify PDMS, and then released the PDMS stamp and substrate from the molds. To sterilize the PDMS stamp and substrate, we exposed them to the UV light for more than 10 h. Afterward, the surface of the PDMS devices was treated with ethanol with 0.5 wt% phosphorylcholine-based (MPC) polymers (NOF Corporation) and incubated at 65°C for 1.5 h in order to block cell adhesion. Finally, we deaerated the PDMS devices in PBS until generation of bubbles had stopped to prevent bubble formation in the fabrication process of the hiPS-CM fibers.

Hydrogel structures with hiPS-CMs were formed using a modified method proposed in a previous report [24]. We placed the anchors on the PDMS substrate, and suspended hiPS-CMs (5×10^7 cells/mL) in a pre-gel solution mixed with the equal amounts of Matrigel (Becton Dickinson) and type-I collagen (Cellmatrix type I-A; Nitta Gelatin, Inc.) (Fig. 1(ii-a, b)). The pre-gel solution was sandwiched using the PDMS stamp and the substrate to pattern the solution in the PDMS stamp and to simultaneously move non-patterned solution to both anchors. After gelation of the solution at 37°C for 10 min, we obtained the striped hydrogel structures containing hiPS-CMs by releasing the PDMS stamp (Fig. 1(ii-c, d)). Finally, we cultured the hiPS-CMs in the striped hydrogel structures using iCell Cardiomyocyte Maintenance Medium. As a result, hiPS-CM fibers were formed between the anchors (Fig. 1(ii-e)). While bodies of the fibers did not adhere to the substrate due to the MPC polymer coating, their edges were fixed to anchors because hiPS-CMs were tangled with the pillars of the anchors. For the formation of narrow and wide hiPS-CM fibers, we used striped hydrogel structures by patterning 7.5 µL and 11 µL of pre-gel solution with 0.5 × 0.5 × 5 mm PDMS stamps and 1.0 × 1.0 × 5 mm PDMS stamps, respectively. Additionally, we prepared hiPS-CM clumps by culturing hiPS-CMs in 1.25 µL hydrogel structures (same volume as 0.5 × 0.5 × 5 mm patterned hydrogel structures without hydrogel on anchors) on the non-adhesive culture dishes for the comparison of gene expression and contractile properties.

Immunostaining and microscopy

For the characterization of hiPS-CMs by immunostaining, samples were washed with PBS, fixed with 4% paraformaldehyde (PFA) (Muto Pure Chemicals Co., Ltd.),

permeabilized with 0.1% Triton X-100 for 20 min, and blocked with 2.5% bovine serum albumin (BSA) (Sigma-Aldrich) overnight. Afterward, we incubated the samples with primary antibodies at 4°C overnight and then with secondary antibodies at room temperature for 2 h. For actin staining, we used 0.1% Alexa Fluor 647-conjugated phalloidin (Thermo Fisher Scientific, Inc.) as the primary antibody, and did not use secondary antibodies. For α-actinin staining, we used 0.1% monoclonal anti-α-actinin antibody (Sigma-Aldrich) as the primary antibody, and 0.1% goat anti-mouse IgG antibody (Thermo Fisher Scientific, Inc.) as secondary antibody. Following this, we rinsed them with PBS and stained cell nuclei with 0.1% Hoechst33342 (Invitrogen).

In order to observe the samples, we used a digital camera with macro lens (EOS Kiss X6i; Canon) for bright-field images, a microscope (IX71N; Olympus) for bright-field and fluorescent microscopy, and laser microscope (LSM780; Zeiss) for confocal microscopy.

Evaluation of iPS-CM orientation

For the quantification of hiPS-CM orientation in the cellular constructs, we applied fast Fourier Transform (FFT) to the images of immunostained actin fibers, and characterized their square regions. Gray scale pixels in the FFT images distributed in circular patterns reflect the actin fiber orientation, and therefore, the radial summed pixel intensities showed the directional distribution of the actin fibers. Based on this distribution, we calculated the orientation values as previous reports [24, 25] to quantify actin fiber orientations (Sup. 1).

Sectional images of the hiPS-CM fiber

For conventional hematoxylin and eosin (H&E) staining, we fixed hiPS-CM fibers with 4% PFA, and dipped them in 30% sucrose solution at 4°C. After we imbedded and frozen the fibers in O.C.T. Compound (Sakura Finetek Japan Co., Ltd.), we cut them in cryostat chamber (Hyrax C25; Carl Zeiss). Frozen sections, 8 μm thick, were mounted on glass slides and further observed. Using the frozen sections, we stained them by terminal deoxynucleotidyl transferase dUTP nick end labeling (TUNEL) with a kit (Apoptosis *in situ* Detection kit; Wako Pure Chemical Industries, Ltd.) for detection of apoptosis.

RT-PCR analysis

We performed RT-PCR analyses in order to confirm the gene expression of cardiac troponin T (cTnT, TNNT2) [26], myosin heavy chain (MHC, MYH6/7) [26], α-actinin (ACTN1) [26], brain natriuretic peptide (BNP, NPPB) [27], and glyceraldehyde-3-phosphate-dehydrogenase (GAPDH, GAPDH) [28]. GAPDH was used as a control for the normalization of gene expression levels. Total mRNA was isolated from the hiPS-CM cellular constructs according to the manufacturer's protocol (TRIzol; Thermo Fisher Scientific, Inc.). We prepared the purified mRNAs to synthesize cDNAs using SuperScript III (Invitrogen). Using the cDNAs and primers listed in Sup. Table 1, we amplified products. The amplified products were labeled using SYBR Green I (TaKaRa Bio Inc.).

Evaluation of contractile properties

To measure contractile frequency and distance of hiPS-CM fibers, we tracked points around center of the fibers with a motion capture software (VW-9000 motion analyser; Keyence Corp.). In the case of the hiPS-CM clumps, we tracked arbitrary points of the clumps using the same software.

We estimated the contractile forces of the hiPS-CM fibers using PDMS substrates with cantilevers. After transferring the hiPS-CM fiber to the PDMS substrate with cantilevers, we observed deformation of the cantilevers caused by hiPS-CM fiber contractions (Fig. 1(ii-f)). Because the contractile forces of the hiPS-CM fibers approximate reaction force measured from the cantilevers, we estimated the contractile forces from the deformation of cantilever according to beam deflection formulas [24]. In this state, friction force between the PDMS substrate and the anchor was negligible because estimated friction force was about 0.2 μN (Sup. 2). To estimate contractile stresses of the hiPS-CM fibers, we assumed that the cross-sectional shapes of the fibers were circle so that the cross-sectional area can be calculated from the width of the hiPS-CM fiber.

To evaluate contractile force of the hiPS-CM fibers under electrical stimulation, we applied electrical pulses to them via gold electrodes. The electrical pulses were generated using a function generator (Agilent) and an amplifier (Mess-Tek Co., Ltd.).

Drug reactivity analysis

To evaluate the drug reactivity of the hiPS-CM cellular constructs, we measured their contractile properties following the treatment with isoproterenol (Sigma-Aldrich) and propranolol (Sigma-Aldrich). Isoproterenol or propranolol were added to iCell Cardiomyocytes Maintenance Medium, which was used for cell culture. The cellular constructs were incubated for 30 min in the medium supplemented with the investigated drugs, and afterward, culture medium was replaced with the fresh medium without drugs.

Statistical analysis

All error bars represent standard deviations. Actin orientation and contractile stress data were compared using one-way analysis of variance (ANOVA) with multiple comparison analysis using a two-sample t-test for each comparison.

Results and discussion

Characteristics of hiPS-CM fibers

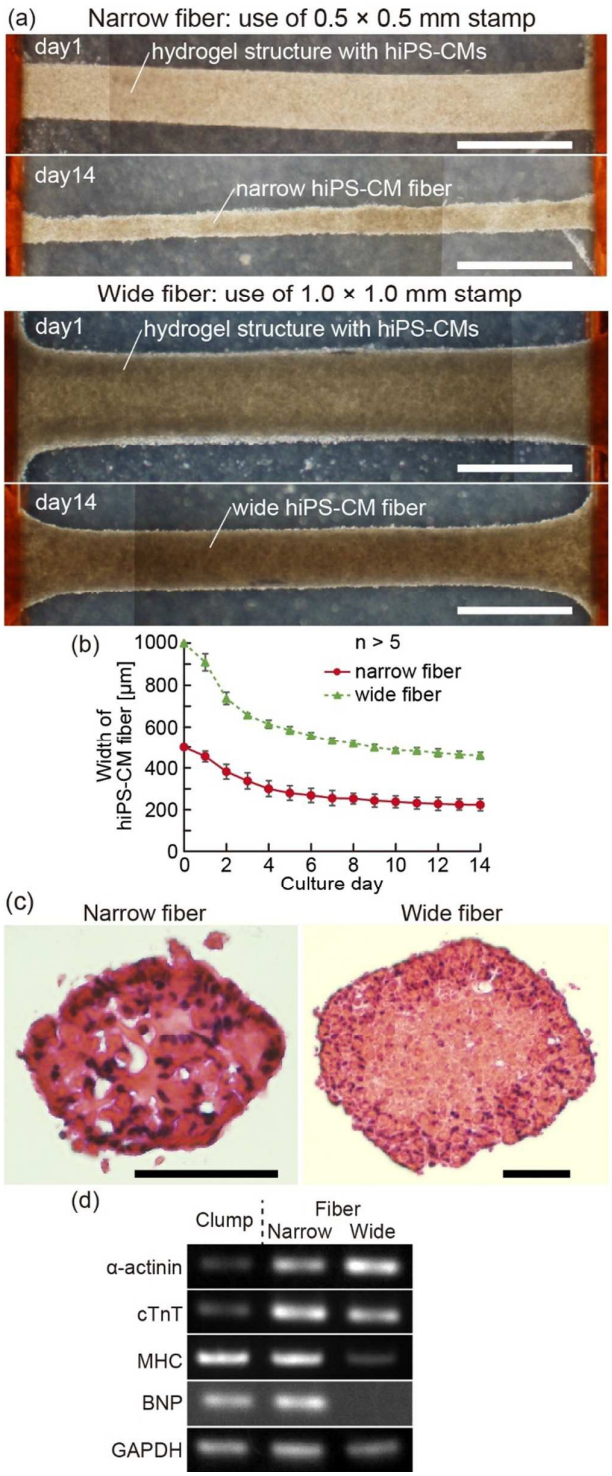

Fig. 2 (a) Formation of narrow and wide hiPS-CM fibers from hydrogel structures with hiPS-CMs, patterned by 0.5 × 0.5 × 5 mm and 1.0 × 1.0 × 5 mm PDMS stamps, respectively. (b) Plot of widths of the hiPS-CM fibers at their central parts in time. (c) Axial sectional images of hiPS-CM fibers stained with H&E. (d) Expression of α-actinin, cTnT, MHC, BNP, and GAPDH in the hiPS-CM fibers and clump. Scale bars show (a) 1 mm and (c) 100 μm.

For the fabrication of hiPS-CM fibers, we first prepared stripe-patterned hydrogel structures with hiPS-CMs by PDMS stamps.

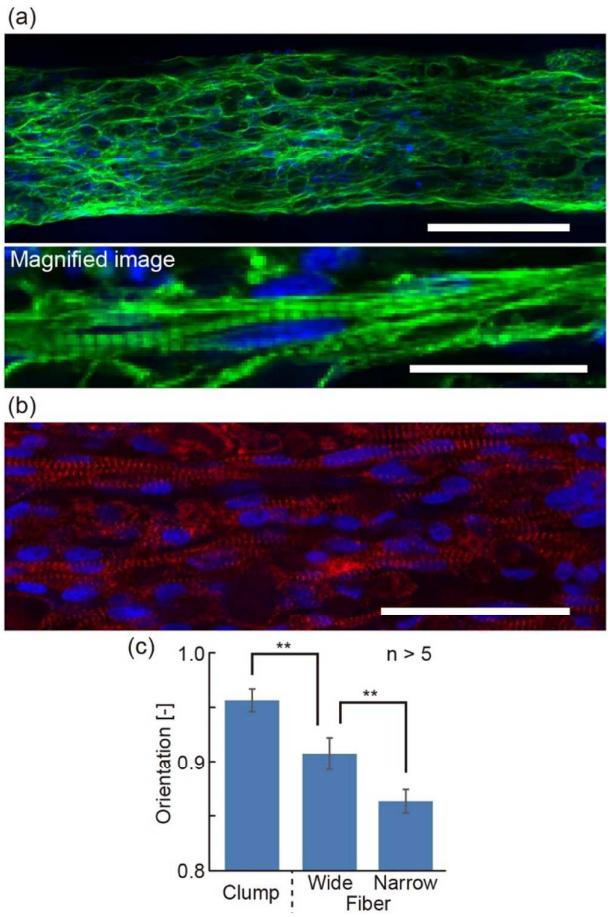

Fig. 3 (a, b) Confocal fluorescent images of the narrow hiPS-CM fiber. (a) Actin (green) and cell nucleus (blue) staining. (b) α-actinin (red) and cell nucleus (blue) staining. (c) Orientation of actin in the wide and narrow hiPS-CM fibers and the hiPS-CM clumps. Lower orientation values indicate higher alignment of the actin (**P<0.01). Scale bars show (a) 100 μm and 20 μm, and (b) 50 μm.

Because the edges of the hydrogel structures were fixed to anchors with pillars, we were able to maintain the length of the structures during culture. Finally, hiPS-CMs adhered each other in the culture, and we succeeded in obtaining hiPS-CM fibers with the edges fixed to the anchors (Fig. 2(a)). Comparing the before-and-after images of these cultures, we confirmed that the width of hiPS-CM fibers gradually decreased with time until it reached approximately one third of the initial hydrogel structure width (Fig. 2(b)). Even though some shape changes were observed during this time, the coefficients of variation of the narrow and wide fiber width were 10% and 3%, respectively, at day 14. This result indicates that our method of hiPS-CM fiber formation allows a high reproducibility of their shapes. In the axial sectional images of hiPS-CM fibers, we observed enucleated cells in the wide fiber differently from the narrow fiber (Fig. 2(c)) and did not observe apoptotic cells in the fibers (Sup. Fig. 1), indicating that central necrosis occurred in the wide hiPS-CM fibers. The result shows that hydrogel structure dimensions influence the viability of the cells in these fibers.

The expression levels of several genes were determined using RT-PCR after 14 days culture of the hiPS-CM fibers and clumps (Fig. 2(d)). The hiPS-CM fibers were shown to express higher levels of cardiac markers such as α-actinin and cTnT than hiPS-CM clump (cellular constructs cultured without anchors), and the narrow hiPS-CM fiber expressed cTnT and MHC higher than the wide hiPS-CM fiber. This result suggests that the narrow-fiber culturing of hiPS-CMs provides appropriate conditions for their maturation. Furthermore, BNP expression, induced when the cardiomyocytes undergo general stress [29, 30], did not differ significantly between the narrow hiPS-CM fiber and hiPS-CM clump. This result indicates that the fixation of hiPS-CM fiber edges does not present a highly general stress for the hiPS-CMs.

In order to evaluate morphology of hiPS-CM fibers, we observed actin and α-actinin arrangement using immunostaining to narrow hiPS-CM fibers (Fig. 3(a, b)) and wide hiPS-CM fibers (Sup. Fig. 2(a, b)). From these images, we confirmed the formation of striped patterns of actin and α-actinin, suggesting formation of sarcomeres. In contrast to this result, the stripes generated in the hiPS-CM clumps were dispersed (Sup. Fig. 2(c, d)). Therefore, the obtained results demonstrate that hiPS-CM fibers have the fundamental morphology required to achieve contractile properties. Furthermore, the immunostaining images showed alignment of hiPS-CMs in the fiber. For quantitative evaluation, we calculated the orientation values of actin fibers from FFT images, which were based on the immunostaining images of the hiPS-CM fibers and the hiPS-CM clumps (Sup. Fig. 2(e)). The orientation values of hiPS-CM fibers were lower than the hiPS-CM clump orientation values, and in particular, the values of narrow hiPS-CM fibers were the lowest, showing that actin was aligned better in the narrow hiPS-CM fibers; low orientation values show better alignment (Fig. 3(c)). We think that the shapes of the hiPS-CM fibers is not only a single factor for the better alignment because it could also cause changes of the nutrient permeability and unidirectional stress of the hiPS-CM fiber. These morphological analyses suggest that preparing the narrow hiPS-CM fibers is an effective way of fabricating highly aligned hiPS-CM cellular constructs that have contractile elements enabling their one-directional contractions.

Contractile properties of hiPS-CM fibers

The hiPS-CM fibers with anchors were able to contract spontaneously along the fiber direction (Sup. Movie 1). In order to confirm the contractile properties of hiPS-CM fibers, we visually evaluated their spontaneous contractions on the PDMS substrate in the culture (Sup. Movie 2). We confirmed that contractile frequencies of hiPS-CM fibers and clumps decreased with time, and the changes of contractile frequencies were the same in all three groups (Fig. 4(a)). Because contractile frequencies of single hiPS-CMs were ranged from 0.3 Hz to 1.8 Hz [6], we think that the hiPS-CM fibers and clumps after 14 days culture show more stable contractile frequencies (narrow hiPS-CM fiber: 0.74 ± 0.14 Hz, wide hiPS-CM fiber: 0.72 ± 0.11 Hz, hiPS-CM clump: 0.59 ± 0.13 Hz) than that of single hiPS-CMs. While, the contractile

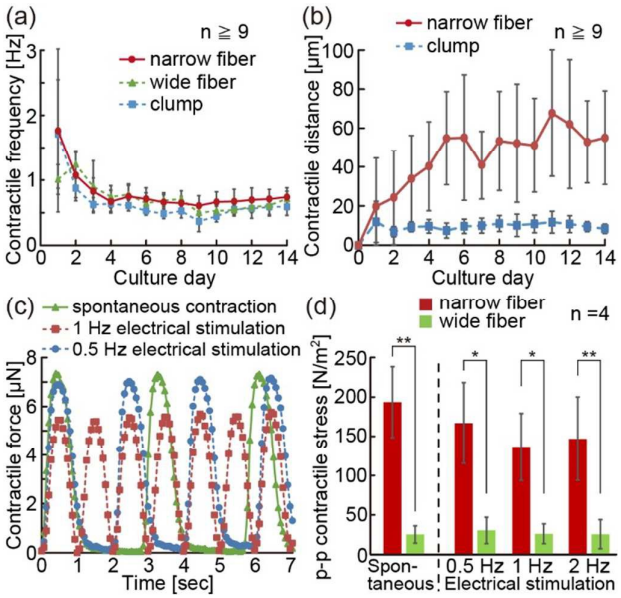

Fig. 4 (a) Changes of spontaneous contractile frequency of the narrow hiPS-CM fibers, the wide hiPS-CM fibers, and the hiPS-CM clumps in culture. (b) Change of spontaneous contractile distance of the narrow hiPS-CM fibers and the hiPS-CM clumps. (c) Temporal variation of contractile force of the narrow hiPS-CM fibers depending on the different contractile conditions (electric field 1.2 V/mm, duration 20 ms). (d) p-p contractile stress of spontaneous contractions and contractions induced by the electrical stimulation of hiPS-CM fibers (electric field 1.2 V/mm, duration 20 ms) (**P<0.01, *P<0.02).

distance of the narrow hiPS-CM fibers increased more than the distance of the clumps, although both of these constructs were fabricated from the same volume of hydrogel structures with hiPS-CMs (Fig. 4(b)). Wide hiPS-CM fibers had wider contractile distance than the clumps as well (Sup. Fig. 3(a, b)), suggesting that the fiber shape and fixation of edges using anchors could enable wider contractions because of hiPS-CM alignment in the fiber. These results indicate that the hiPS-CM fibers achieved wide contractile distances without changing the contractile frequencies of hiPS-CMs.

Additionally, because electrical stimulation triggers the contractions of the heart muscle in vivo, we electrically stimulated hiPS-CM fibers and investigated their reactivity. For this experiment, we transferred the hiPS-CM fibers on the PDMS substrate with cantilevers. The contractions of the hiPS-CM fibers were induced spontaneously or using electrical stimulations (Sup. Movie 3). The obtained results confirm that the contractile frequencies of the hiPS-CM fibers were synchronized with frequencies of electrical stimulations similar to conventional reports using hES-CM and hiPS-CM constructs [18, 23]. In this state, we additionally estimated the contractile force of the hiPS-CM fibers from the deformations of the cantilevers generated by the motions of the fibers. Because these measurements were based on cantilever deformation movies, the changes in contractile forces were measured using the frame rate speed of the movies (Fig. 4(c)). The result shows that electrical stimulations controlled contractile frequencies of the hiPS-CM fibers as well. Using the system, we were able to measure peak-to-peak (p-p) value of contractile forces

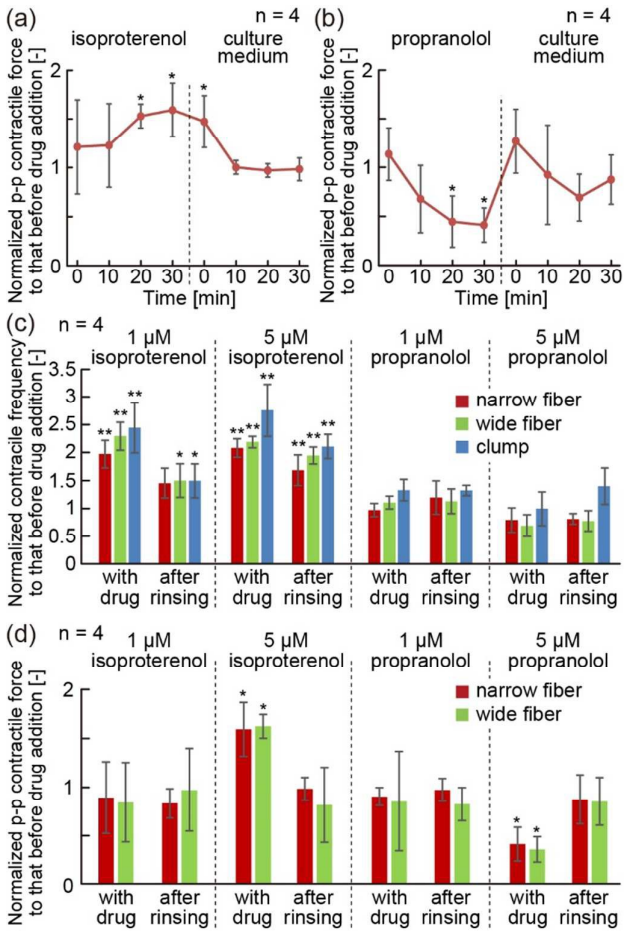

Fig. 5 (a, b) Temporal changes of p-p contractile force of the hiPS-CM fibers upon the treatment with (a) 5 μM of isoproterenol and (b) 5 μM of propranolol, and after the removal of these drugs. (c) Contractile frequency of the hiPS-CM fibers and clumps 30 min after the addition or removal of isoproterenol and propranolol. (d) p-p contractile force of the hiPS-CM fibers 30 min after the addition or removal of isoproterenol and propranolol. (**P<0.02, *P<0.05, showing relations to data before addition of drug.)

during the spontaneous contractions and contractions induced by electrical stimulation (Sup. Fig. 3(c, d)), and calculated p-p contractile stress of the hiPS-CM fibers from the p-p contractile force and estimated cross-sectional area. As a result, p-p contractile stress of the narrow fiber was shown to be higher than that of the wide fiber (Fig. 4(d)), suggesting that high alignment and viability of hiPS-CMs in the narrow fibers increase their contractile strength. Thus, we believe that the formation of the narrow hiPS-CM fiber provides the appropriate conditions for the improvement of contractile properties of hiPS-CM cellular constructs.

Drug reactivity of hiPS-CM fibers

In order to demonstrate drug reactivity of hiPS-CM fibers, we used isoproterenol and propranolol. In the human body, isoproterenol is known to increase contractile force and heart rate upon binding to β-receptors of CMs. In contrast, propranolol blocks β-receptors, and decreases contractile force and heart rate. Using the hiPS-CM fiber system, we were able to detect an increase in p-p contractile force that followed the addition of isoproterenol, and a decrease in p-p contractile force after the addition of propranolol (Fig. 5 (a, b)). Additionally, 30 min after the removal of these drugs, their contractile force returned to the initial values before addition of the drugs. These results indicate that the hiPS-CM fibers show reversible drug reactivity.

Furthermore, we quantitatively compared the contractile properties of the narrow and wide hiPS-CM fibers with the hiPS-CM clumps, following the drug treatments. The changes in contractile frequencies showed the same tendency in all investigated groups — they increased following the isoproterenol treatment and decreased after the treatment with propranolol (Fig. 5(c)). Moreover, p-p contractile force of the hiPS-CM fibers increased and decreased depending on the type of the applied drug as well (Fig. 5(d)). The narrow and wide hiPS-CM fibers showed the same drug reactivity, indicating that the drug reactivity of the hiPS-CMs does not depend on orientation and contractile strength of hiPS-CMs. In contrast to this result, the contractile distances of the hiPS-CM clumps did not change according to the type of the applied drug (Sup. Fig. 4), indicating that the contractile distance cannot be used as a substitute index of contractile force during drug testing. These experiments indicate that hiPS-CM fibers provide suitable conditions for the evaluation of hiPS-CM contractile properties in the studies investigating their pathology and drug reactivity.

Conclusion

In this study, we developed the method for the construction of hiPS-CM fibers by culturing hiPS-CMs in hydrogel structures shaped with PDMS stamps. Using this method, we have achieved a highly reproducible morphology of hiPS-CM fibers. Furthermore, the shapes of PDMS stamps allowed the control of hiPS-CMs orientation in the fiber, and highly aligned hiPS-CMs were formed in the fibers when PDMS stamp with narrow channel was used. Due to improvement of alignment and viability of hiPS-CMs in the narrow fibers, the narrow shape led to an increase in contractile stress of the hiPS-CM fibers. Moreover, the hiPS-CM fibers changed their contractile frequency and p-p contractile force depending on the type of the applied drugs. The changes of contractile properties follows efficacy of the applied drugs in the human bodies. Therefore, we believe that the measurements of changes in the contractile properties of hiPS-CM fibers will be useful tool for drug development studies, as the first-in-human test.

Acknowledgements

The authors would like to thank Tomoharu Osada (LSI Medience Corp.) for valuable discussions and Maiko Onuki and Midori Kato Negishi for their technical assistance.

References

1 C J. C. Ralphe, and W. J. de Lange, *Trends Cardiovas. Med.*, 2013, **23**, 27-32.
2 X. L. Yang, L. Pabon, and C. E. Murry, *Circ. Res.*, 2014, **114**, 511-523.
3 H. Masumoto, T. Ikuno, M. Takeda, H. Fukushima, A. Marui, S. Katayama, T. Shimizu, T. Ikeda, T. Okano, R. Sakata, and J. K. Yamashita, *Scientific Reports*, 2014, **4**, 6716.
4 N. Huebsch, P. Loskill, M. A. Mandegar, N. C. Marks, A. S. Sheehan, Z. Ma, A. Mathur, T. N, Nguyen, J. C. Yoo, L. M. Judge, C. I. Spencer, A. C. Chukka, C. R. Russell, P. L. So, B. R. Conklin, and K. E. Healy, *Tissue Eng. Part C-Me.*, 2015, **21**, 467-479.
5 A. Ahola, A. L. Kiviaho, K. Larsson, M. Honkanen, K. Aalto-Setala, and J. Hyttinen, *Biomed. Eng. Online.*, 2014, **13**, 39.
6 T. Hayakawa, T. Kunihiro, T. Ando, S. Kobayashi, E. Matsui, H. Yada, Y. Kanda, J. Kurokawa, and T. Furukawa, *J Mol. Cell. Cardiol.*, 2014, **77**, 178-191.
7 M. Fujiwara, P. S. Yan, T. G. Otsuji, G. Narazaki, H. Uosaki, H. Fukushima, K. Kuwahara, M. Harada, H. Matsuda, S. Matsuoka, K. Okita, K. Takahashi, M. Nakagawa, T. Ikeda, R. Sakata, C. L. Mummery, N. Nakatsuji, S. Yamanaka, K. Nakao, and J. K. Yamashita, *Plos One* 2011, **6**, e16734.
8 K. Asakura, S. Hayashi, A. Ojima, T. Taniguchi, N. Miyamoto, C. Nakamori, C. Nagasawa, T. Kitamura, T. Osada, Y. Honda, C. Kasai, H. Ando, Y. Kanda, Y. Sekino, and K. Sawada, *J Pharmacol. Tox. Met.*, 2015, **75**, 17-26.
9 M. L. Rodriguez, B. T. Graham, L. M. Pabon, S. J. Han, C. E. Murry, and N. J. Sniadecki, *J. Biomech. Eng.*, 2014, **136**, 051005.
10 K. Morishima, Y. Tanaka, M. Ebara, T. Shimizu, A. Kikuchi, M. Yamato, T. Okano, and T. Kitamori, *Sensor Actuat. B-Chem.*, 2006, **119**, 345-350.
11 Y. Tanaka, K. Morishima, T. Shimizu, A. Kikuchi, M. Yamato, T. Okano, and T. Kitamori, *Lab Chip*, 2006, **6**, 230-235.
12 Y. Zhao, and X. Zhang, *Sensor Actuat. A-Phys.*, 2006, **125**, 398-404.
13 A. Kajzar, C. M. Cesa, N. Kirchgessner, B. Hoffmann, and R. Merkel, *Biophys. J.*, 2008, **94**, 1854-1866.
14 N. L. Tulloch, V. Muskheli, M. V. Razumova, F. S. Korte, M. Regnier, K. D. Hauch, L. Pabon, H. Reinecke, and C. E. Murry, *Circ. Res.*, 2011, **109**, 47-59.
15 R. E. Akins, D. Rockwood, K. G. Robinson, D. Sandusky, J. Rabolt, and C. Pizarro, *Tissue. Eng. Pt. A.*, 2010, **16**, 629-641.
16 A. Mihic, J. Li, Y. Miyagi, M. Gagliardi, S. H. Li, J. Zu, R. D. Weisel, G. Keller, and R. K. Li, *Biomaterials*, 2014, **35**, 2798-2808.
17 Z. Ma, S. Koo, M. A. Finnegan, P. Loskill, N. Huebsch, N. C. Marks, B. R. Conklin, C. P. Grigoropoulos, and K. E. Healy, *Biomaterials*, 2014, **35**, 1367-1377.
18 S. S. Nunes, J. W. Miklas, J. Liu, R. Aschar-Sobbi, Y. Xiao, B. Y. Zhang, J. H. Jiang, S. Masse, M. Gagliardi, A. Hsieh, N. Thavandiran, M. A. Laflamme, K. Nanthakumar, G. J. Gross, P. H. Backx, G. Keller, and M. Radisic, *Nat. Methods*, 2013, **10**, 781-787.
19 I. Vollert, M. Seiffert, J. Bachmair, M. Sander, A. Eder, L. Conradi, A. Vogelsang, T. Schulze, J. Uebeler, W. Holnthoner, H. Redl, H. Reichenspurner, A. Hansen, and T. Eschenhagen, *Tissue Eng. Pt. A.*, 2014, **20**, 854-863.
20 J. Y. Xi, M. Khalil, N. Shishechian, T. Hannes, K. Pfannkuche, H. M. Liang, A. Fatima, M. Haustein, F. Suhr, W. Bloch, M. Reppel, T. Saric, M. Wernig, R. Janisch, K. Brockmeier, J. Hescheler, and F. Pillekamp, *Faseb J.*, 2010, **24**, 2739-2751.
21 I. C. Turnbull, I. Karakikes, G. W. Serrao, P. Backeris, J. J. Lee, C. Q. Xie, G. Senyei, R. E. Gordon, R. A. Li, F. G. Akar, R. J. Hajjar, J. S. Hulot, and K. D. Costa, *Faseb J.*, 2014, **28**, 644-654.
22 A. Stoehr, C. Neuber, C. Baldauf, I. Vollert, F. W. Friedrich, F. Flenner, L. Carrier, A. Eder, S. Schaaf, M. N. Hirt, B. Aksehirlioglu, C. W. Tong, A. Moretti, T. Eschenhagen, and A. Hansen, *Am. J. Physiol. Heart Circ. Physiol.*, 2014, **306**, H1353-H1363.
23 M. N. Hirt, J. Boeddinghaus, A. Mitchell, S. Schaaf, C. Bornchen, C. Muller, H. Schulz, N. Hubner, J. Stenzig, A. Stoehr, C. Neuber, A. Eder, P. K. Luther, A. Hansen, and T. Eschenhagen, *J. Mol. Cell Cardiol.*, 2014, **74**, 151-161.
24 Y. Morimoto, M. Kato-Negishi, H. Onoe, and S. Takeuchi, *Biomaterials*, 2013, **34**, 9413-9419.
25 D. Kiriya, M. Ikeda, H. Onoe, M. Takinoue, H. Komatsu, Y. Shimoyama, I. Hamachi, and S. Takeuchi, *Angew. Chem. Int. Ed.*, 2011, **51**, 1553-1557.
26 R. Koninckx, A. Daniels, S. Windmolders, F. Carlotti, U. Mees, P. Steels, J. L. Rummens, M. Hendrikx, and K. Hensen, *Cell. Mol. Life Sci.*, 2011, **68**, 2141-2156.
27 J. Borlak, and T. Thum, *Faseb J.*, 2003, **17**, 1592-1608.
28 S. Miura, K. Mitsui, T. Heishi, C. Shukunami, K. Sekiguchi, J. Kondo, Y. Sato, and Y. Hiraki, *Exp. Cell Res.*, 2010, **316**, 775-788.
29 J. P. Goetze, C. Christoffersen, M. Perko, H. Arendrup, J. F. Rehfeld, J. Kastrup, and L. B. Nielsen, *Faseb J.*, 2003, **17**, 1105-1107.
30 S. Kudoh, H. Akazawa, H. Takano, Y. Z. Zou, H. Toko, T. Nagai, and I. Komuro, *Prog. Biophys. Mol. Bio.*, 2003, **82**, 57-66.